JOURNAL OF MATERIALS SCIENCE 24 (1989) 2898–2902

The distribution of graphitic microcrystals and the sensitivity of their Raman bands to strain in SiC fibres

R. J. DAY, VALERIE PIDDOCK, R. TAYLOR, R. J. YOUNG, M. ZAKIKHANI
Manchester Materials Science Centre, UMIST, Grosvenor Street, Manchester M1 7HS, UK

Raman spectra have been obtained from commercially produced silicon carbide fibres. These fibres contain significant amounts of carbon and silica. Two types of observation have been made. In the first case fibre sections were examined to determine the size of the graphitic microcrystals. Secondly, since it is known that the Raman bands of certain types of fibre including carbon fibres exhibit strain dependence, the effect of strain on the graphitic component of silicon carbide fibres has been examined.

1. Introduction

It has been demonstrated [1–3] that Raman spectroscopy is an excellent technique for following the deformation of high-modulus fibres, and it has been found that the frequencies of a number of Raman bands in polymeric and carbon fibres are shifted by the application of tensile and compressive stresses. Results have been obtained for several types of high-modulus polymer fibre [1, 2] and a range of carbon fibres [3] derived from different precursors. The shifts in these Raman frequencies reflect the fact that in these high-modulus materials, macroscopic deformation leads directly to bond stretching.

Raman spectra have been reported for a number of silicon carbide polymorphs [4]. The cubic 3C polytype gives rise to strong peaks at $972\,\mathrm{cm}^{-1}$, corresponding to the longitudinal optic phonon peak, and at $796\,\mathrm{cm}^{-1}$, due to the transverse optic phonon line. A low-intensity peak is observed at $796\,\mathrm{cm}^{-1}$ in the spectrum of the high-temperature hexagonal 6H form of silicon carbide together with a strong line at $789\,\mathrm{cm}^{-1}$.

Spectra have also been obtained for silicon carbide fibres derived from a polycarbosilane precursor [5]. Such fibres contain not only silicon carbide, but also significant amounts of free carbon and silica, the actual proportions depending on the pyrolysis temperature [4]. X-ray diffraction studies have indicated that the silicon carbide component has a face-centred cubic morphology [5]. High-resolution transmission electron microscopy of silicon carbide fibres has yielded an average grain size for the silicon carbide which is dependent on heat treatment temperature, ranging from ~ 1 to 20 nm [5]. Carbon was observed within the fibres as uniformly distributed microcrystallites surrounded by silicon carbide [6]. Raman spectroscopy has confirmed the existence of microcrystalline silicon carbide, carbon and silica in SiC fibres [5].

Raman spectra obtained from fibres heat-treated below 1400° C are very different from those of fibres which have experienced higher temperatures. Below 1400° C, broad Raman lines occur at around 400, 750, 1350 and $1600\,\mathrm{cm}^{-1}$. A sharp peak is present at $795\,\mathrm{cm}^{-1}$ in the spectrum of fibres heat-treated at higher temperatures (> 1500° C). The peaks at 1350 and $1600\,\mathrm{cm}^{-1}$ which are due to the small crystals of graphite are then suppressed. Graphitic materials generally exhibit a Raman band at about $1580\,\mathrm{cm}^{-1}$. This has been attributed to an E_{2g} mode of the infinite crystal lattice. In the case of polycrystalline carbon, a second, lower frequency peak is observed at $1360\,\mathrm{cm}^{-1}$. This is due to the grain boundary regions. The relative intensities of the two peaks offer an indirect measure of carbon grain size [7].

Silicon carbide fibres heated to 1200 to 1300° C exhibit optimum tensile strength [8]. This is consistent with the observed microstructure. The fine dispersion of carbon microcrystals is thought to suppress grain growth of the surrounding silicon carbide. During heat treatment, carbon is lost by oxidation but this loss is compensated by continued precipitation from the carbon-rich silicon carbide. However, above 1500° C evolution of CO results in the removal of carbon which is not replaced by further precipitation. Consequently growth of the silicon carbide grains is no longer constrained and the resultant grain growth above 1500° C leads to a reduction in strength.

In this study we have used Raman microscopy to examine the internal structure of SiC fibres. Strain dependence in the Raman spectrum has also been investigated, utilizing the more intense graphitic peaks.

2. Experimental procedure

Two types of Raman measurement have been made on Nicalon (Nippon Carbon Co. Ltd, Japan) silicon carbide fibres, examples of which are shown in Fig. 1. These fibres were derived from a polycarbosilane precursor. In the first case, the distribution of the carbon within the fibres was examined as a function of

0022–2461/89 $03.00 + .12

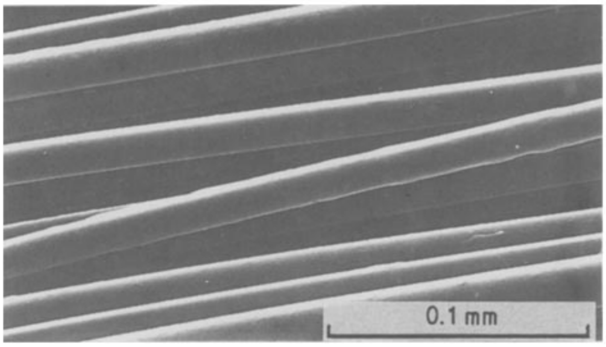

Figure 1 Scanning electron micrograph of the silicon carbide fibres.

distance into the fibre. This was achieved by mounting fibres longitudinally in an epoxy resin. Under the Raman microscope, fibres could be selected which had been exposed to different depths after grinding and polishing. Some fibres were also mounted at an angle to the surface of the specimen so that an oblique section could be examined, and some were embedded perpendicular to the surface in order to investigate transverse sections.

In the second type of measurement, single fibres of silicon carbide were fixed on to a purpose-built straining rig using aluminium foil tabs and a cyanoacrylate adhesive. The fibres were extended in steps of approximately 0.1% using a micrometer built into the straining rig. The latter was placed on the stage of a modified Nikon optical microscope which had a vernier scale allowing the fixed ends of the fibres to be observed and the gauge length to be measured. This was approximately 10 mm for the experiments reported here. The Raman system consisted of the modified microscope coupled to a Spex 1403 monochromator. The 488 nm line of an air-cooled argon ion laser was used to excite the Raman spectrum. A spectral bandpass of approximately 10 cm^{-1} was used and spectra were obtained from 1 to 2 μm diameter regions of individual fibres. Measurements were concentrated on the bands in the Raman spectrum due to the graphitic carbon in the fibres, since these are significantly stronger than those due to the silicon carbide.

Stress–strain curves for individual fibres were obtained using a Model 1121 Instron testing machine with a crosshead speed of 1 mm min^{-1} and a gauge length of 50 mm. A 5 N load cell was fitted and measurements were made using 1 N full scale deflection.

A bundle of fibres was examined by wide-angle X-ray scattering using a flat-plate transmission geometry and nickel-filtered Cu$K\alpha$ radiation. Fibre diameters were determined by scanning electron microscopy.

3. Results and discussion

3.1. Fibre structure

Spectra taken from two fibres, one sectioned transversely and the other cut obliquely, are presented in Fig. 2. The two spectra are very similar, both exhibiting broad, relatively intense peaks at 1336 and 1601 cm^{-1} together with a broad peak or group of peaks in the region 800 to 900 cm^{-1}. The higher-frequency peaks

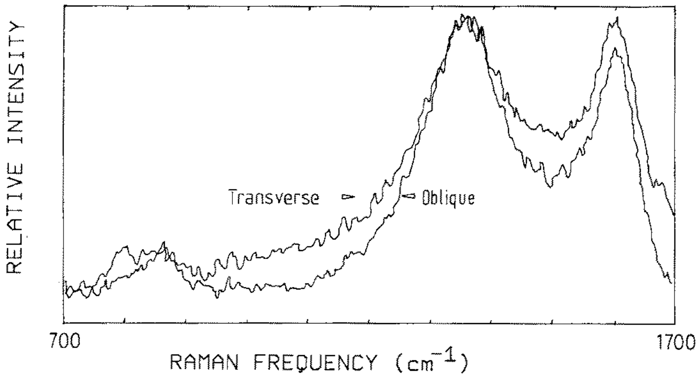

Figure 2 Raman spectra of a silicon carbide fibre taken at the centre of a transverse section and at the centre of an oblique section angled at 18° to the fibre axis.

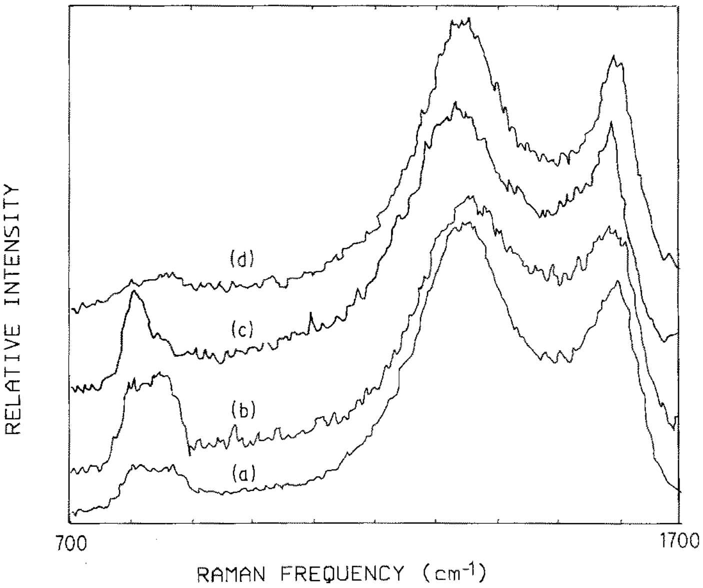

Figure 3 Raman spectra of silicon carbide fibres taken at increasing depths into the fibres: (a) 0 μm, (b) 0.2 μm, (c) 0.9 μm, (d) 3.8 μm.

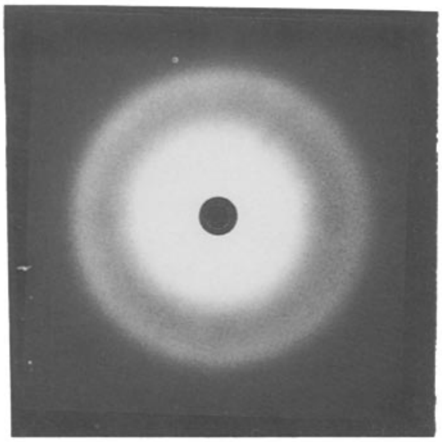

Figure 4 Wide-angle X-ray scattering pattern obtained from silicon carbide fibres.

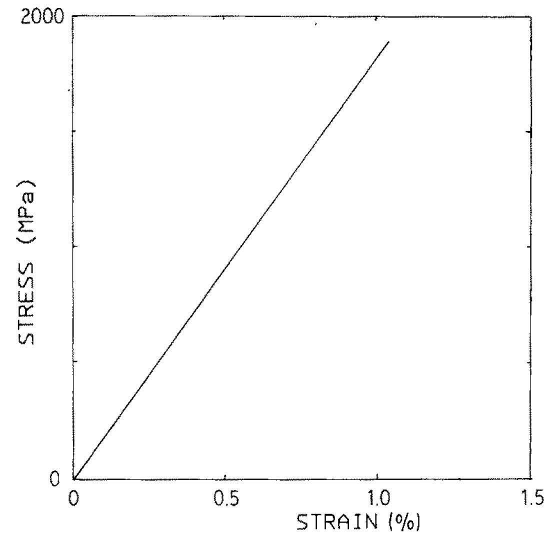

Figure 5 Typical stress–strain curve obtained for a single silicon carbide fibre.

are due to the graphite distributed throughout the fibre, whilst the silicon carbide gives rise to the lower-frequency, less intense bands. Since the efficiency of Raman scattering from graphite has been estimated to be one-tenth that of silicon carbide [5], the ratio of peak heights is not a direct measure of the amounts of carbon and silicon carbide present in the fibre.

Spectra obtained from longitudinal fibre sections are presented in Fig. 3. The depths of these sections were calculated from the measured average fibre diameter of 14.5 μm and from the exposed width. The traces correspond to fibre sections approximately 0.2, 0.9 and 3.8 μm into the fibres, together with a spectrum taken from the surface of the fibre. The shallower sections gave rise to similar spectra in terms of peak positions and relative intensities, although the band due to silicon carbide was broader for the section near the surface and may indeed be a multiple peak. The relative heights of the peaks in the Raman spectrum obtained from the section closest to the centre of the fibre were appreciably different from those in the spectra taken from nearer the surface, the silicon carbide band appearing weaker at the centre of the fibre. At the surface itself the graphite peaks were again relatively strong. This indicates a higher concentration of carbon nearer the centre and on the surface of the fibre. Average grain sizes estimated using the results reported by Tuinstra and Koenig [7] are given in Table I. It would appear that there is little variation in graphite crystallite size between fibres examined longitudinally, transversely and obliquely, crystallite diameters being in the range 3.5 to 4.1 nm. The wide-angle X-ray pattern (Fig. 4) is similar in appearance to those reported by Yajima *et al.* [9]. The diffuse nature and broadening of the rings indicate a high degree of polycrystallinity and relatively small crystal size in the fibres.

3.2 Fibre deformation

The deformation of the silicon carbide fibres was followed using both standard mechanical testing and Raman microscopy. A typical stress–strain curve for a single Nicalon fibre is shown in Fig. 5. The stress–strain curve shows a linear increase in strain with applied stress and the Young's modulus obtained from these measurements is 185 ± 24 GPa which is within the range quoted elsewhere [8] for similar fibres. The strength of the fibres was found to be 1.9 ± 0.2 GPa.

It was also found that the position of the 1601 cm^{-1} Raman band is sensitive to the level of applied strain. This is illustrated in Fig. 6, which shows detail of this band both unstrained and at a strain of 2%. It can be seen that the tensile strain causes a significant shift of the peak to lower frequency. The position of the peak as a function of applied strain for several different fibres is plotted in Fig. 7. It can be seen that there is a linear shift in position of the peak with extension, reflecting the linearity of the stress–strain curve in Fig. 5. The slope of the least-squares fit of the line in Fig. 7 is 6.6 cm^{-1} (% strain)$^{-1}$. It should be remembered that the 1601 cm^{-1} band is due to the graphitic

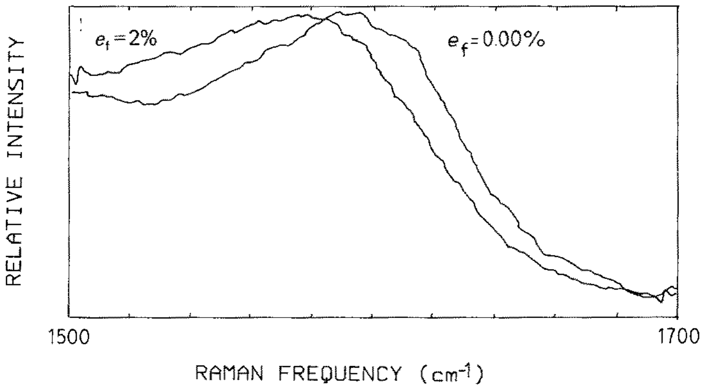

Figure 6 Detail of Raman spectra obtained from an unstrained fibre and the same fibre strained to 2% elongation.

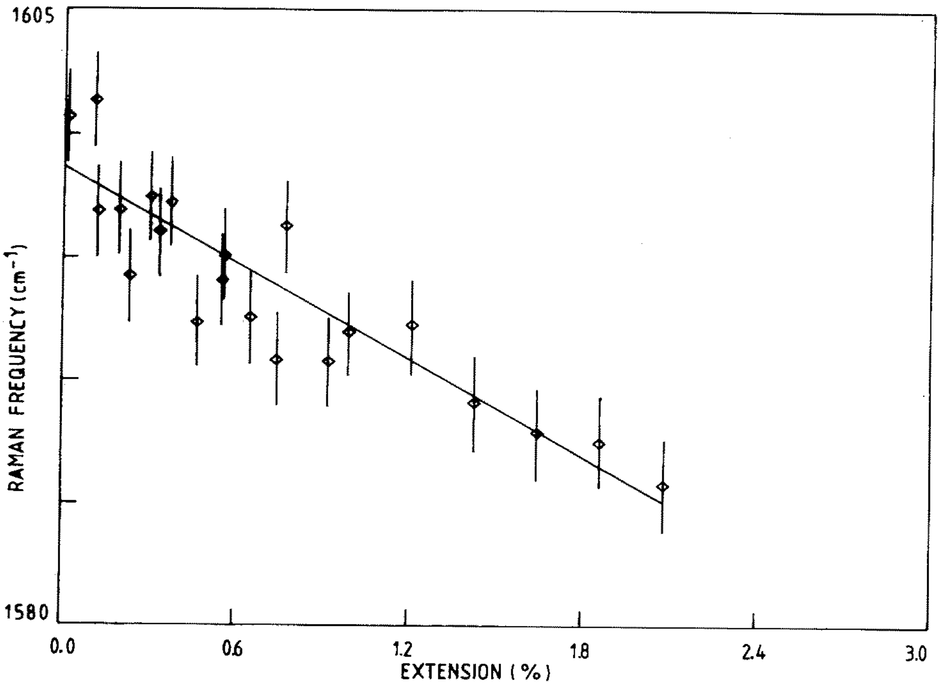

Figure 7 Variation of the 1601 cm^{-1} Raman band with strain for several fibres.

component of the fibre and the shift in this band is a reflection of the deformation of the graphitic component of the fibres. Initial measurements of the 1336 cm^{-1} band showed that this peak is comparatively insensitive to strain.

The behaviour demonstrated in Figs 6 and 7 is very similar to that of other fibres such as polydiacetylenes [2], rigid-rod polymer fibres [1], aromatic polyamide fibres [10] and carbon fibres [3] in which the Raman bands are all sensitive to the level of strain. In all of these high-modulus fibres, macroscopic deformation results directly in bond stretching which is reflected in changes in peak positions in the Raman spectra. It appears that a phenomenon has been discovered which is of general application to most types of high-modulus fibre.

Previous studies [11, 12] have shown that the phenomenon can be used to follow the detailed micromechanics of deformation of fibres within a composite. This is because Fig. 7 is effectively a strain-gauge calibration curve, enabling local strains in 1 to 2 μm regions to be measured from a fibre under any general state of stress or strain in a composite with a transparent matrix. Recent work [13] has shown that values of fibre critical length and matrix shrinkage can be determined for model polydiacetylene–epoxy composites. It is highly likely that similar measurements could be made for other types of fibre such as SiC in a suitable matrix, and work is currently progressing in this direction.

TABLE I Grain size of graphitic microcrystals

Section	I_{1336}/I_{1601}	L_a (nm)
Longitudinal (surface)	1.28	3.5
Longitudinal (0.2 μm subsurface)	1.17	3.7
Longitudinal (0.9 μm subsurface)	1.17	3.7
Longitudinal (3.8 μm subsurface)	1.22	3.6
Transverse	1.09	4.1
Oblique	1.16	3.8

4. Conclusions

In this paper Raman microscopy has been used to examine the behaviour of the graphitic component of silicon carbide fibres, both as a function of distance through the fibres and of strain. Our findings on the size of the graphite microcrystals indicate that there is little variation throughout the fibre in the directions examined. The ratio of the 1610 and 1336 cm^{-1} peaks yields a size for these microcrystals of 3.5 to 4.1 nm in the *a* lattice direction, using the calibration of ratio of Raman intensities against crystallite size produced by Tuinstra and Koenig [7].

The sensitivity to strain of the 1601 cm^{-1} band of these graphitic microcrystals appears to be linear with strain, giving a shift in the 1601 cm^{-1} band of 6.6 cm^{-1} (% strain)$^{-1}$. The band at 1336 cm^{-1} was relatively insensitive to strain.

Acknowledgements

The authors wish to thank the SERC, UMIST, DuPont and the EEC Brite Programme for their financial support. The Nicalon fibres were supplied by Société Européene de Propulsion, Bordeaux, France.

References

1. R. J. DAY, I. M. ROBINSON, M. ZAKIKHANI and R. J. YOUNG, *Polymer* **28** (1987) 1833.
2. C. GALIOTIS, R. J. YOUNG and D. N. BATCHELDER R, *J. Polym. Sci. Polym. Phys. Edn* **21** (1983) 2483.
3. I. M. ROBINSON, M. ZAKIKHANI, R. J. DAY and R. J. YOUNG, *J. Mater. Sci. Lett.* **6** (1987) 1212.
4. H. OKUMURA, E. SAKUMA, H. J. LEE, H. MUKAIDA, S. MISAWA, K. ENDO and S. YOSHIDA, *J. Appl. Phys.* **61** (1987) 1134.
5. Y. SASAKI, Y. NISHINA, M. SATO and K. OKAMURA, *J. Mater. Sci.* **22** (1987) 443.
6. S. YAJIMA, K. OKAMURA, T. MATSUZAWA, Y. HASEGAWA and T. SHISHIDO, *Nature* **279** (1979) 706.
7. F. TUINSTRA and J. L. KOENIG, *J. Compos. Mater.* **4** (1970) 492.

8. S. YAJIMA, in "Handbook of Composites", Vol. 1 (Elsevier, 1985) p. 228.
9. S. YAJIMA, K. OKAMURA, J. HAYASHI and M. OMORI, *J. Amer. Ceram. Soc.* **59** (1978) 324.
10. C. GALIOTIS, I. M. ROBINSON, R. J. YOUNG, B. J. E. SMITH and D. N. BATCHELDER, *Polym. Commun.* **26** (1985) 354.
11. R. J. YOUNG, R. J. DAY, M. ZAKIKHANI and I. M. ROBINSON, *Compos. Sci. Technol.* **34** (1989) 243.
12. I. M. ROBINSON, R. J. YOUNG, C. GALIOTIS and D. N. BATCHELDER, *J. Mater. Sci.* **22** (1987) 3642.
13. I. M. ROBINSON, PhD thesis, University of London (1987).

Received 20 June
and accepted 27 September 1988